Res Chem Intermed
DOI 10.1007/s11164-015-2003-8

Ionic liquid immobilized on Fe_3O_4 nanoparticles: a magnetically recyclable heterogeneous catalyst for one-pot three-component synthesis of 1,8-dioxodecahydroacridines

Heshmatollah Alinezhad[1] · Mahmood Tajbakhsh[1] · Neda Ghobadi[1]

Received: 17 January 2015 / Accepted: 5 March 2015

Abstract A magnetically recoverable nanocatalyst based on 1-methylimidazolium hydrogen sulfate ionic liquid has been synthesized by reaction of 1-methylimidazole with 3-(trimethoxysilyl)propyl chloride group, leading to formation of 1-methyl-3-(triethoxysilyl)propyl imidazolium chloride ([pmim]Cl). The ionic liquid was anchored onto silica-coated magnetic Fe_3O_4 particles, and Cl^- anion exchange by treatment with H_2SO_4 afforded the corresponding immobilized ionic liquid MNP-[pmim]HSO_4. The synthesized catalyst was characterized by various techniques such as Fourier-transform infrared (FT-IR) spectroscopy, X-ray diffraction (XRD) analysis, scanning electron microscopy (SEM), transmission electron microscopy (TEM), (differential) thermogravimetry (TG/DTG), CHN analysis, and vibrating-sample magnetometry (VSM), revealing the superparamagnetic nature of the particles. From electron microscopy (SEM and TEM) studies it can be inferred that the particles were mostly spherical in shape with average size of 20 nm. The loading amount of ionic liquid supported on the magnetic particles was indicated to be 0.98 mmol/g by the results of elemental and thermogravimetric analyses (CHN and TG). The catalytic activity of the supported ionic liquid was examined in synthesis of 1,8-dioxodecahydroacridines by condensation reaction of cyclic diketones with aromatic aldehydes and ammonium acetate or primary amines under solvent-free conditions. The catalyst could be easily recovered by applying an external magnetic field and reused for at least nine runs without deterioration in catalytic activity.

Keywords Ionic liquids · Magnetic nanoparticles · 1,8-Dioxodecahydroacridines · Heterogeneous catalyst · One-pot

✉ Heshmatollah Alinezhad
alinezhad_n@yahoo.com; heshmat@umz.ac.ir

[1] Faculty of Chemistry, University of Mazandaran, PO Box 47415, Babolsar, Iran

Published online: 10 April 2015

Introduction

Synthesis of organic compounds at high yields is one of the most important subjects in modern drug discovery. Organic reactions should be fast and facile, and the target products should be easily separated and purified in high yields [1]. From this point of view, multicomponent reactions (MCRs) have received a great deal of interest for the implementation of new processes and new synthetic strategies [2]. One-pot multicomponent reaction strategies offer significant advantages over conventional linear-type syntheses by virtue of their convergence, productivity, facile execution, and high yield [3]. MCRs often comply with the principles of green chemistry, which emphasizes the development of environmentally benign chemical processes and technologies in terms of economy of steps as well as meeting the many stringent criteria of ideal organic synthesis [4, 5].

1,8-Dioxodecahydroacridines are polyfunctionalized 1,4-dihydropyridine (DHP) derivatives [6], being very important compounds because of their pharmacological properties [7]. Acridine derivatives have been used to synthesize labeled conjugates with medicinal action, and peptides, proteins, and nucleic acids [8], and used as antimalarial agents [9] and in chemotherapy for cancer [10]. Acridine derivatives are frequently employed in industry, especially for production of dyes [11]. In literature, synthesis of acridines has been carried out in organic solvents in the presence of triethylbenzylammonium chloride (TEBAC) [12], *p*-dodecylbenzenesulfonic acid (DBSA) [13], proline [6], Amberlyst-15 [14], ammonium chloride or $Zn(OAc)_2{\cdot}2H_2O$ or L-proline [15], under microwave irradiation [16], ionic liquids [17, 18], using ceric ammonium nitrate (CAN) in polyethylene glycol (PEG) [19] and silica-bonded *S*-sulfonic acid [20].

Although many of the above-mentioned methods are effective, some of them suffer from drawbacks such as prolonged reaction time and tedious preparation processes in the synthesis of the catalyst [17], low yields with anilines containing electron-withdrawing groups [13], time-consuming methods for catalyst recovery, harsh reaction conditions, etc. Therefore, to overcome such shortcomings, it is highly desirable to introduce a green and highly efficient method applying a reusable, nonhazardous catalyst for efficient synthesis of 1,8-dioxodecahydroacridines.

Green chemistry approaches are significant due to the reduction in by-products, reaction waste, and energy cost [21]. Room-temperature ionic liquids (RTILs) as homogeneous catalysts [22] are widely emerging as green solvents, catalysts, and reagents for use in organic synthesis [23] because of their unique properties, such as low vapor pressure, high chemical and thermal stability, solvating ability, nonflammability, acidic or basic character, and recyclability [24]. Although these compounds possess such promising advantages, their widespread practical application is still hampered by various drawbacks which lead to economical and environmental problems. High viscosity limits their mass transfer during catalytic reactions and also makes their handling difficult. Moreover, use of relatively large amounts of ionic liquids and their homogeneity cause toxicological concerns and environmental problems [25]. These problems and also the preference in the

chemical industry to use heterogeneous catalysts can be addressed by immobilization of ILs on solid supports [26].

Among the different reported methods for preparation of supported ionic liquids, magnetic nanoparticles (MNPs) have recently appeared as a new type of catalyst support because of their good stability and facile separation [27]. Magnetic catalysts can be recycled using an external magnetic field for reuse in subsequent reactions. Among such materials, nano-Fe_3O_4 has attracted much attention due to its unique physical properties such as high surface area, excellent thermal and chemical stability, low toxicity, and potential applications. Owing to these properties and attractive features, Fe_3O_4 has been used as a promising support for ILs [28].

In this context, we synthesized IL of 1-methyl-3-(trimethoxysilyl)propyl imidazolium hydrogen sulfate immobilized on nano-Fe_3O_4 (MNP-[pmim]HSO_4) (Scheme 1) and used it as a recyclable catalyst for synthesis of decahydroacridines (Scheme 2). This synthetic protocol avoids the above-mentioned problems and also has advantages including use of easily prepared catalyst, high efficiency, short reaction time, and simple work-up procedure.

Experimental

General information

Chemical materials were purchased from Merck and Aldrich chemical companies and used without further purification. All solvents were distilled, dried, and purified using standard procedures. Samples were analyzed using a Vector 22 FT–

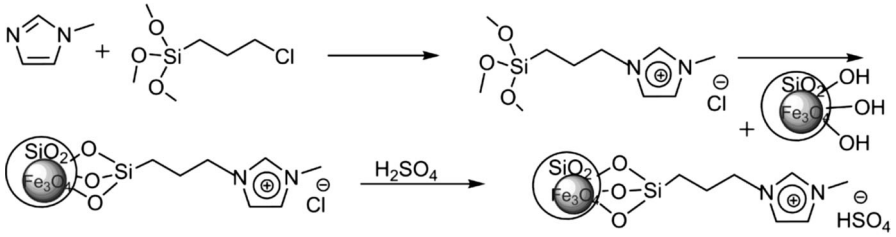

Scheme 1 Immobilization of ionic liquid on the surface of nanoparticle

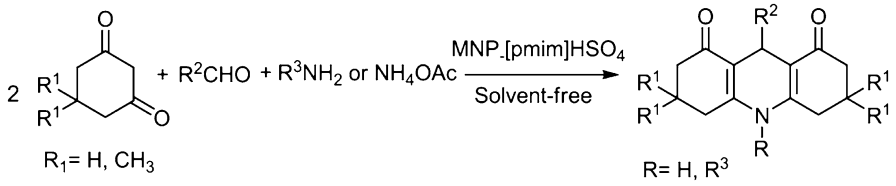

Scheme 2 One-pot synthesis of 1,8-dioxodecahydroacridines

IR spectrometer (Bruker) in KBr matrix. Nuclear magnetic resonance (NMR) spectra were recorded on a Bruker DRX-400 AVANCE instrument (400.1 MHz for ^{1}H, 100.6 MHz for ^{13}C) with $CDCl_3$ as solvent. Chemical shifts (δ) are given in parts per million (ppm) relative to tetramethylsilane (TMS), and coupling constants (J) are reported in hertz (Hz). Elemental analyses were performed using a Heraeus CHNS/O-Rapid analyzer. Thermogravimetric analysis (TGA) was recorded on a Stanton Redcraft STA-780 (London, UK). XRD was carried out on a PHILIPS X'Pert PRO diffractometer using a Cu K_α source ($\lambda = 1.5418$ Å). Field-emission SEM (FESEM) images were obtained on a Hitachi S-1460 field-emission scanning electron microscope using an alternating-current (AC) voltage of 15 kV. Transmission electron microscopy (TEM) experiments were conducted for the TEM images in Fig. 5a, c using a Zeiss-EM10C at accelerating voltage of 80 kV and for Fig. 5b on a Philips EM 208 electron microscope. Magnetic measurements were performed using vibrating-sample magnetometry (VSM, MDK, model 7400) analysis. Melting points were measured on an Electrothermal 9100 apparatus.

General procedure for synthesis of catalyst

Silica-coated magnetite nanoparticles (Fe_3O_4@SiO_2) were prepared according to the reported method [29]. Then, ionic liquid of 1-methyl-3-(trimethoxysilyl)propyl imidazolium chloride ([pmim]Cl) was synthesized according to the reported method [30]. In the next step, [pmim]Cl was anchored onto the silica-coated magnetite nanoparticles and heated at 90 °C for 16 h. Afterwards, unreacted ionic liquid was removed by 24 h extraction with boiling dichloromethane, and the material (MNP-[pmim]Cl) was dried under high vacuum. Finally, for Cl^- anion exchange, MNP[pmim]Cl (1 g) was suspended in 20 ml dry CH_2Cl_2. Under vigorous stirring, concentrated H_2SO_4 (1.3 mmol, 98 %) was introduced dropwise at 0 °C. Then the mixture was warmed up to room temperature and refluxed for 48 h. The mixture was cooled, filtered, and dried to give supported hydrogen sulfate ionic liquid of MNP-[pmim]HSO_4.

General procedure for synthesis of 1,8-dioxodecahydroacridine derivatives

MNP-([pmim]HSO_4) (0.01 g, 1 mol%) was added to a stirred mixture of aldehyde (1.0 mmol), cyclic diketone (2.0 mmol), and ammonium acetate or primary amines (1 mmol), and the resulting mixture was stirred at 80 °C for appropriate time. The progress of the reaction was monitored by thin-layer chromatography (TLC). After completion of the reaction, EtOAc (10 ml) was added to the cooled reaction mixture. The catalyst was separated by an external magnet, washed with EtOAc, dried, and reused in consecutive runs under the same reaction conditions. Evaporation of the organic solvent under reduced pressure gave the crude products. Finally, pure products were obtained by recrystallization by aqueous EtOH. The products were characterized by IR, ^{1}H and ^{13}C NMR spectra, and melting point.

Results and discussion

Characterization of catalyst

The external surface of the magnetite nanoparticles was coated with silica (Fe_3O_4@SiO_2) to improve the chemical stability and prevent further aggregation of MNPs. 1-Methyl-3-(trimethoxysilyl)propyl imidazolium chloride anchored onto the solid support via cation–anion interaction remained unbound to the surface of Fe_3O_4@SiO_2. Ion exchange of Cl^- anions using H_2SO_4 afforded MNP-[p-mim]HSO_4. FT-IR spectroscopy was used to provide evidence for immobilization of IL onto the solid support. FT-IR spectra of MNPs (a), MNP@SiO_2 (b), [pmim]Cl (c), MNP-[pmim]Cl (d), and MNP-[pmim]HSO_4 (e) are shown in Fig. 1. Pure

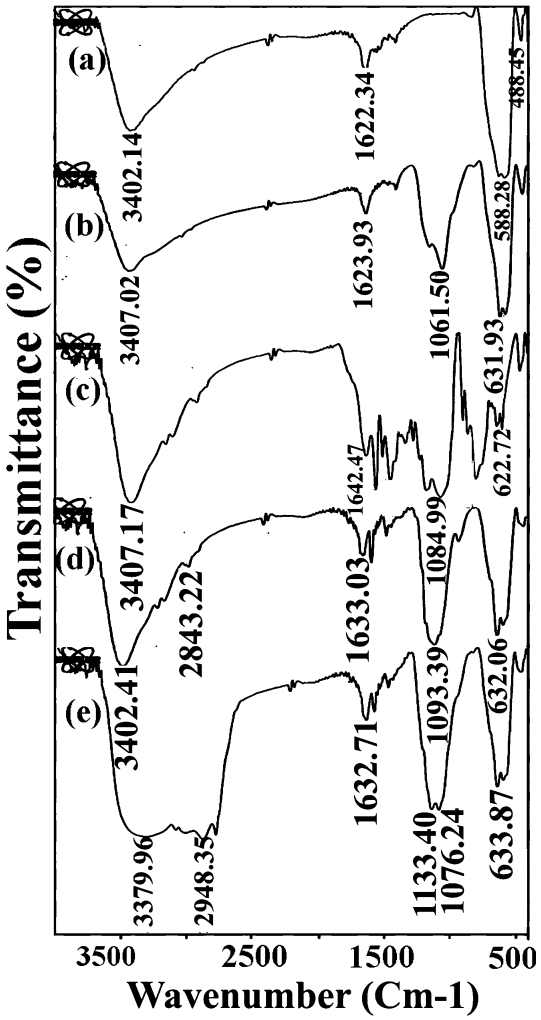

Fig. 1 FTIR spectra of MNPs (**a**), MNP@SiO_2 (**b**), [pmim]Cl (**c**), MNP-[pmim]Cl (**d**), and MNP-[pmim]HSO_4 (**e**)

magnetic nanoparticles demonstrate peaks at approximately 590 cm^{-1} corresponding to Fe–O stretching and at 3420 cm^{-1} related to stretching vibration of physisorbed water and potentially surface hydroxyls, and the deformation vibration absorption peak at 1630 cm^{-1} belonging to O–H bond (Fig. 1a) [31].

The other FT-IR spectra shown in Fig. 1b, d, e confirm the presence of the magnetic core in the prepared nanomaterials. In Fig. 1b, in addition to characteristic peaks of MNP, the absorption peak present at 1061 cm^{-1} is most probably due to stretching vibration of framework and Si–O–Si groups [32]. In the FT-IR spectrum of 1-methyl-3-(trimethoxysilyl)propyl imidazolium chloride IL ([pmim]Cl, Fig. 1c), characteristic peaks corresponding to stretching vibrations of C=N and C–N appear at 1642 and 1588 cm^{-1}, respectively. For MNP-[pmim]Cl (Fig. 1d), the band at 1093 cm^{-1} is assigned to asymmetric vibration of (Si–O-Si), whereas the observed C–H stretching band present at 2955 cm^{-1} and the band at 3402 cm^{-1} are attributed to symmetric and asymmetric stretching vibrations of OH groups, in good agreement with reported FT-IR data [30]. In the spectrum of MNP-[pmim]HSO_4 (e), signals corresponding to O=S=O asymmetric and symmetric stretching modes appear at 1133 and 1076 cm^{-1}, respectively, together with the broad OH stretching absorption around 2800–3380 cm^{-1}, confirming exchange of Cl^- ions with HSO_4^- ions.

The crystalline structure of MNP-[pmim]HSO_4 was characterized by X-ray diffraction (XRD, Fig. 2). The diffraction pattern showed characteristic peaks at 2θ values of 30.2°, 35.6°, 43.3°, 53.7°, 57.2°, and 62.8°, being assigned to (220), (311), (400), (422), (511), and (440) crystal planes of the Fe_3O_4 cubic lattice, respectively,

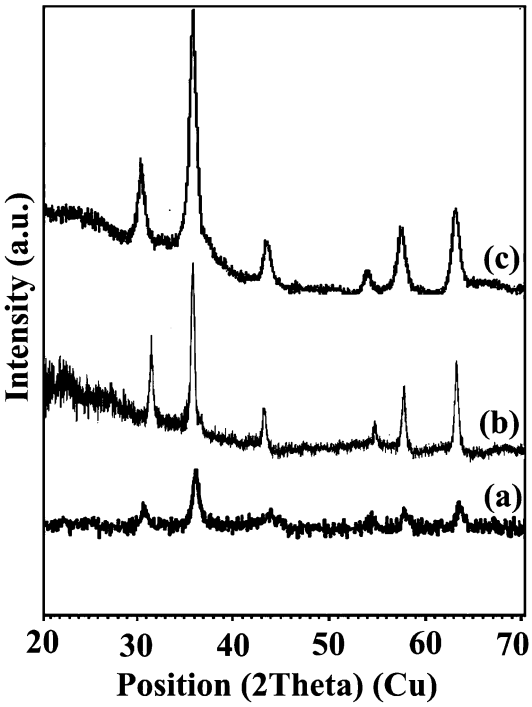

Fig. 2 XRD pattern of MNP (**a**), MNP@SiO_2 (**b**), and MNP-[pmim]HSO_4 (**c**)

in agreement with the standard Fe_3O_4 Joint Committee on Powder Diffraction Standards (JCPDS) card no. 19-0629.

In the XRD pattern of MNP@SiO_2 (Fig. 2b), in comparison with the pure MNP peaks (Fig. 2a), we could see peaks for amorphous silica at $2\theta = 20$–$30°$. This demonstrates successful coating of Fe_3O_4 nanoparticles with SiO_2. The XRD pattern of MNP-[pmim]HSO_4 (Fig. 2c) is very similar to the XRD pattern of MNP@SiO_2, confirming that coating with the SiO_2 layer (b) or immobilization of the ionic liquid (c) does not change the structure of the Fe_3O_4 nanoparticles [36]. The average crystallite size was calculated for MNP-[pmim]HSO_4 to be 10 nm using the Scherrer equation with $K = 0.9$ and $\lambda = 0.154$ nm.

The TGA analyses for MNP@SiO_2 (a) and MNP-[pmim]HSO_4 (b) are shown in Fig. 3. For MNP@SiO_2, the weight loss around 200 °C is attributed exclusively to physically adsorbed water molecules and surface hydroxyl groups on the magnetite surface. For MNP-[pmim]HSO_4, weight loss within 0–160 °C (2.75 %) is due to physically adsorbed moisture, whereas the major weight losses occur at 160–340 °C (10.03 %) and 360–650 °C (11.83 %), being related to decomposition of 1-methyl-3-propylimidazolium groups grafted onto the MNP@SiO_2 surface. According to the TGA results, the amount of IL supported on Fe_3O_4 was evaluated to be 0.98 mmol/g.

The particle sizes of MNP-[pmim]HSO_4 and MNP@SiO_2 were evaluated using scanning electron microscopy (SEM). The SEM images (Fig. 4) showed floccules without regular structure. On the other hand, the shape of these particles was mostly spherical and their surface was nonsmooth, resulting in an increase in the surface areas of these particles. In these cases, the average diameter of MNP-[pmim]HSO_4 was 20–30 nm. As can be seen from the TEM images (Fig. 5), the size of MNPs and MNP@SiO_2 (b) nanoparticles was about 10 and 15 nm, respectively, and for MNP-[pmim]HSO_4 (c) it was around 20 nm. The particles were spherical in shape with some agglomeration, which is obvious because of the magnetic nature of the particles; the TEM image of MNP@SiO_2 nanoparticles clearly shows the dark nano-Fe_3O_4 core surrounded by a grey silica shell and uniform coating by SiO_2 (Fig. 5b).

The loading amount of IL ([pmim]HSO_4) grafted onto the MNPs was also quantified via the C, H, and N contents as determined by elemental analysis (C:

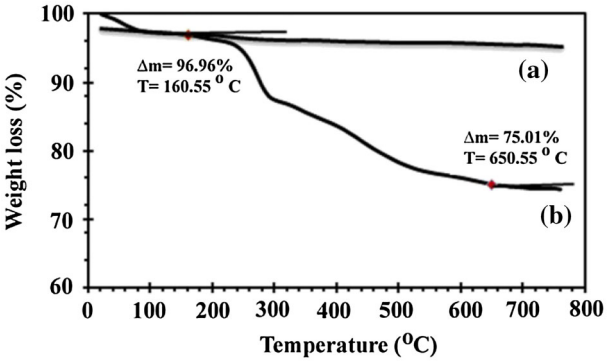

Fig. 3 TGA thermograms of (**a**) MNP@SiO_2 and (**b**) MNP-[pmim]HSO_4

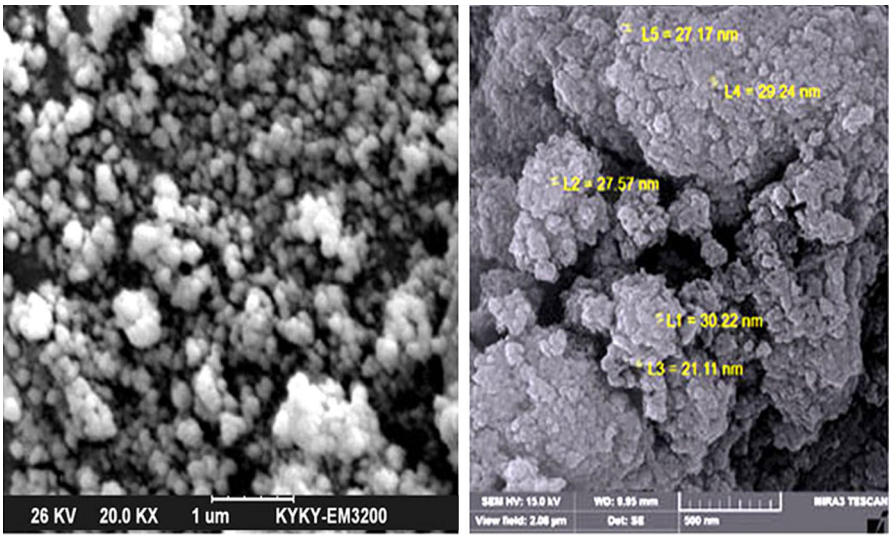

Fig. 4 SEM images of MNP@SiO_2 (*left*) and MNP-[pmim]HSO_4 (*right*)

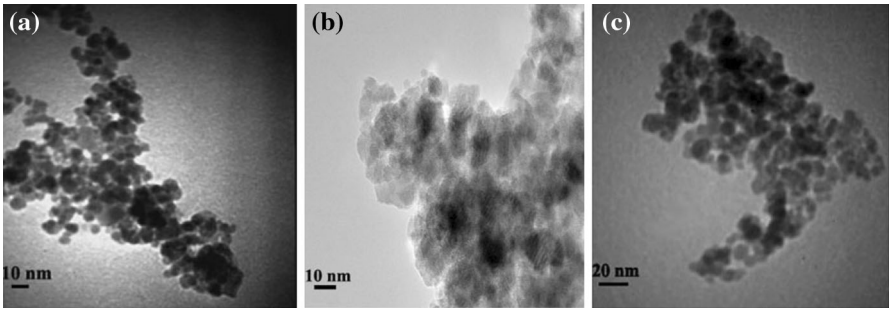

Fig. 5 TEM images of MNP (**a**), MNP@SiO_2 (**b**), and MNP-[pmim]HSO_4 (**c**)

8.36 %; H: 1.32 %; N: 2.67 %; S: 3.19 %). The ratio of C/N content (3.13) was very near to the theoretical calculation (3.00). The content of sulfur further confirmed the amount of loading. The loading level of IL (0.99 mmol/g) was determined based on the chloride content in MNP-[pmim]Cl by the titration method [33]. The loading as evaluated by the titration method was in good agreement with the results obtained from TGA and conventional elemental analysis.

Magnetic hysteresis measurements were carried out for both MNP@SiO_2 and MNP-[pmim]HSO_4 by VSM at 300 K, sweeping the field from −8000 to +8000 Oe. As shown in Fig. 6, the magnetic saturation values for MNP@SiO_2 and MNP-[pmim]HSO_4 reached 57.2 and 43.6 emu/g, respectively. The hysteresis loop for the particles was completely reversible, showing that the nanoparticles exhibit superparamagnetic characteristics and the particles did not show any coercivity. The reversibility in the graph confirms that no aggregation was imposed

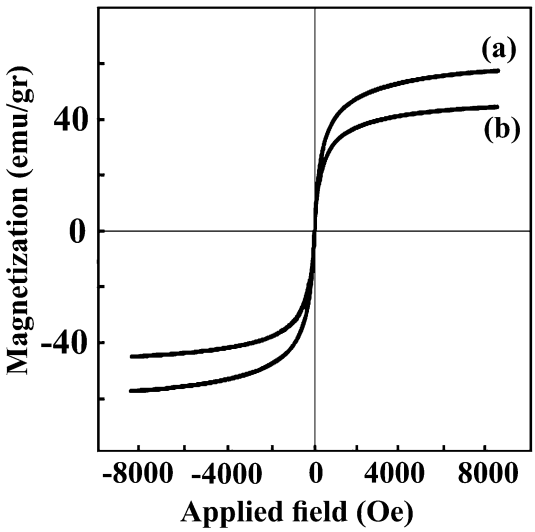

Fig. 6 VSM curves of MNP@SiO_2 (**a**) and MNP-[pmim]HSO_4 (**b**)

on the nanoparticles by the magnetic fields. The lower magnetic saturation of the latter nanoparticles suggests successful coating of [pmim]HSO_4 ionic liquid on the MNP@SiO_2 nanoparticles.

After characterization of the catalyst (MNP-[pmim]HSO_4), its catalytic activity was investigated in synthesis of 1,8-dioxodecahydroacridines via one-pot reaction of cyclic diketones, aromatic aldehydes, and ammonium acetate or primary amines under solvent-free conditions. To optimize the reaction conditions such as the molar ratio of catalyst, temperature, and solvent, reaction of 5,5-dimethyl-1,3-cyclohexanedione (2 mmol), aniline (1 mmol), and benzaldehyde (1 mmol) was chosen as a model reaction (Table 1). First, three separate reactions were examined in the absence of any catalyst and in the presence of MNP@SiO_2 and MNP-[pmim]Cl; the results of these studies showed that trace amount of the desired product was formed (Table 1, entries 14–16). Similar reaction in the presence of imidazolium hydrogen sulfate ([Hmim]HSO_4) as a nonsupported IL gave the desired product in 40 % yield (Table 1, entry 17).

For optimization of the solvent, the model reaction was carried out in the presence of 1 mol% MNP-[pmim]HSO_4 in protic solvents such as H_2O, MeOH, and EtOH; the results indicated that low yield of the product was obtained (Table 1, entries 1–3). However, in the case of aprotic solvents such as CH_2Cl_2, ethyl acetate, and acetonitrile, this reaction did not give a reasonable yield of the expected product (Table 1, entries 4–6). However, the model reaction under solvent-free conditions gave a suitable yield of the product (Table 1, entries 8–13). Since the best solvent from the green chemistry point of view is no solvent due to the minimization of environmental effects and the combination of solvent-free conditions with multicomponent reaction has been shown to be a powerful strategy for making complex molecular structures, we chose it as the optimal reaction condition.

Regarding the catalyst ratio, it seems that increasing the amount of catalyst did not improve the product yield further, whereas decrease of the catalyst led to a

Table 1 Optimization of reaction conditions

Entry	Catalyst (mol%)	Solvent	Temperature (°C)	Time (h:min)	Yield (%)[a]
1	MNP-[pmim]HSO_4 (1)	H_2O	80	4	30
2	MNP-[pmim]HSO_4 (1)	EtOH	Reflux	4	60
3	MNP-[pmim]HSO_4 (1)	MeOH	Reflux	4	25
4	MNP-[pmim]HSO_4 (1)	CH_3CN	80	4	45
5	MNP-[pmim]HSO_4 (1)	EtOAc	Reflux	4	40
6	MNP-[pmim]HSO_4 (1)	CH_2Cl_2	Reflux	4	20
7	MNP-[pmim]HSO_4 (1)	Toluene	80	4	35
8	MNP-[pmim]HSO_4 (0.6)	Solvent free	80	1:30	80
9	MNP-[pmim]HSO_4 (0.8)	Solvent free	80	00:50	80
10	MNP-[pmim]HSO_4 (1)	Solvent free	80	00:10	97
11	MNP-[pmim]HSO_4 (1.2)	Solvent free	80	00:10	95
12	MNP-[pmim]HSO_4 (1)	Solvent free	60	00:50	85
13	MNP-[pmim]HSO_4 (1)	Solvent free	100	00:10	95
14	MNP-[pmim]Cl (1)	Solvent free	80	4	20
15	MNP@SiO_2 (0.01 g)	Solvent free	80	4	20
16	–	Solvent free	80	4	–
17	[Hmim]HSO_4 (1)	Solvent free	80	3	40

Conditions: benzaldehyde:aniline:5,5-dimethyl-1,3-cyclohexanedione (1:1:2)

[a] Isolated yields

reduction in product yield (entries 8, 9, and 11). The model reaction was also carried out at different temperatures under solvent-free condition (entries 10, 12, and 13). Finally, it was found that the best yield of the product was obtained at 80 °C under solvent-free conditions in the presence of 1 mol% [pmim]HSO_4 (Table 1, entry 10).

After optimizing the reaction conditions (Table 1, entry 10), the generality of the method was investigated by using structurally different aldehydes and amines or ammonium acetate under the optimized reaction conditions (Table 2). It is clear from this table that both electron-donating and electron-withdrawing groups on the aromatic ring of the aldehyde and amine are tolerated in this reaction, with high yields of the corresponding products being obtained in short reaction times (Table 2, entries 1–20). Reaction with NH_4OAc also gave high yields of the expected products (entries 21–24). It is interesting to mention that, in all cases, only acridines were separated from the reaction mixture without formation of any xanthene derivatives.

Recovery and reuse of a catalyst is highly preferable for a catalytic process. In this regard the recyclability of MNP-[pmim]HSO_4 was investigated in the model reaction of 5,5-dimethyl-1,3-cyclohexanedione (2 mmol), aniline (1 mmol), and benzaldehyde (1 mmol) under optimized reaction conditions. After completion of the reaction, EtOAc was added to the reaction mixture and the whole amount of MNP-[pmim]HSO_4 simply separated from the product by an external magnet.

Table 2 Synthesis of 1,8-dioxo-9,10-diaryl decahydroacridine derivatives

Entry	Aldehyde	Amine	R^1	Time (min)	Yield[a]	M.p. (°C)	Ref.
1	C_6H_5–	C_6H_5–	CH_3	10	97	253–255	[14]
2	4-ClC_6H_4–	C_6H_5–	CH_3	10	95	244–246	[34]
3	4-$MeOC_6H_4$	C_6H_5–	CH_3	20	90	260–262	[19]
4	C_6H_5–	4-MeC_6H_4	CH_3	25	92	262–264	[13]
5	4-ClC_6H_4–	4-MeC_6H_4	CH_3	15	96	271–173	[33]
6	4-MeC_6H_4	4-MeC_6H_4	CH_3	20	90	296–298	[13]
7	4-$MeOC_6H_4$	4-MeC_6H_4	CH_3	25	87	281–283	[13]
8	C_6H_5–	4-$MeOC_6H_4$	CH_3	20	92	215–216	[17]
9	4-ClC_6H_4–	4-$MeOC_6H_4$	CH_3	25	96	251–253	[17]
10	4-MeC_6H_4	4-$MeOC_6H_4$	CH_3	20	90	237–239	[17]
11	4-$MeOC_6H_4$	4-$MeOC_6H_4$	CH_3	25	92	212–214	[17]
12	4-$MeOC_6H_4$	4-ClC_6H_4–	CH_3	15	95	280–282	[35]
13	4-MeC_6H_4–	4-ClC_6H_4–	CH_3	20	92	237–239	[20]
14	4-ClC_6H_4–	4-ClC_6H_4–	CH_3	25	95	294–296	[20]
15	C_6H_5–	C_6H_5–	H	30	90	274–276	[6]
16	4-ClC_6H_4–	C_6H_5–	H	25	87	292–293	[19]
17	4-$MeOC_6H_4$	C_6H_5–	H	30	92	270–272	[35]
18	C_6H_5–	4-MeC_6H_4	H	25	90	203–205	[6]
19	4-$MeOC_6H_4$–	4-$MeOC_6H_4$	H	30	92	265–266	[36]
20	4-$MeOC_6H_4$	4-MeC_6H_4	H	25	95	235–238	[6]
21	C_6H_5–	NH_4OAc	CH_3	20	95	190–192	[37]
22	4-ClC_6H_4–	NH_4OAc	CH_3	15	90	>300	[37]
23	4-MeC_6H_4	NH_4OAc	CH_3	25	87	268–270	[37]
24	4-$MeOC_6H_4$	NH_4OAc	CH_3	20	87	270–272	[37]

Condition: cyclic diketones:amines:aldehydes:MNP-[pmim]HSO_4 (2:1:1:0.01), 80 °C, solvent-free

[a] Yields refer to isolated pure products

The recovered catalyst was washed with ethyl acetate, dried at room temperature, and reused for the next reaction. In fact, the magnetic property of MNP-[pmim]HSO_4 facilitates efficient recovery of the catalyst from the reaction mixture during the work-up procedure. The recycled catalyst was reused for nine consecutive trials without significant loss of catalytic activity in comparison with fresh catalyst (Fig. 7).

According to documents reported in the literature [13, 34], a plausible mechanism for the formation of acridines is presented in Scheme 3. It is assumed that activation of carbonyl groups in one molecule of 1,3-diketone (**1**) and aldehyde (**2**) by MNP([pmim]HSO_4 as a Brønsted acid facilitates the aldol condensation reaction to generate intermediate **3**. Michael reaction of active methylene group of the second molecule of 1,3-diketone with intermediate **3** and removal of one water molecule gives intermediate **5**. Nucleophilic attack of amine group to activate

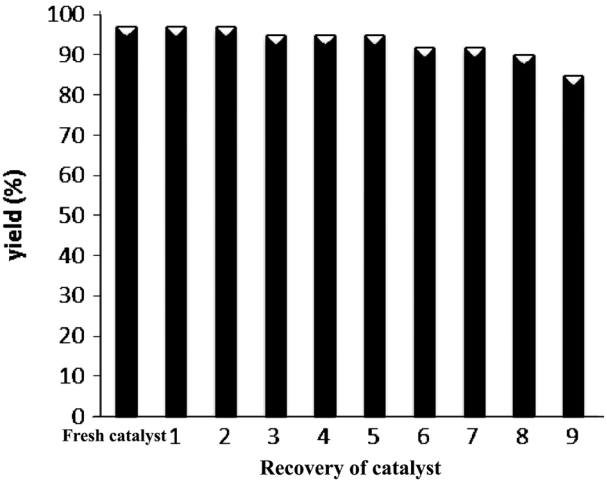

Fig. 7 Recycling of MNP-[pmim]HSO_4 for the model reaction under optimized conditions at 10 min

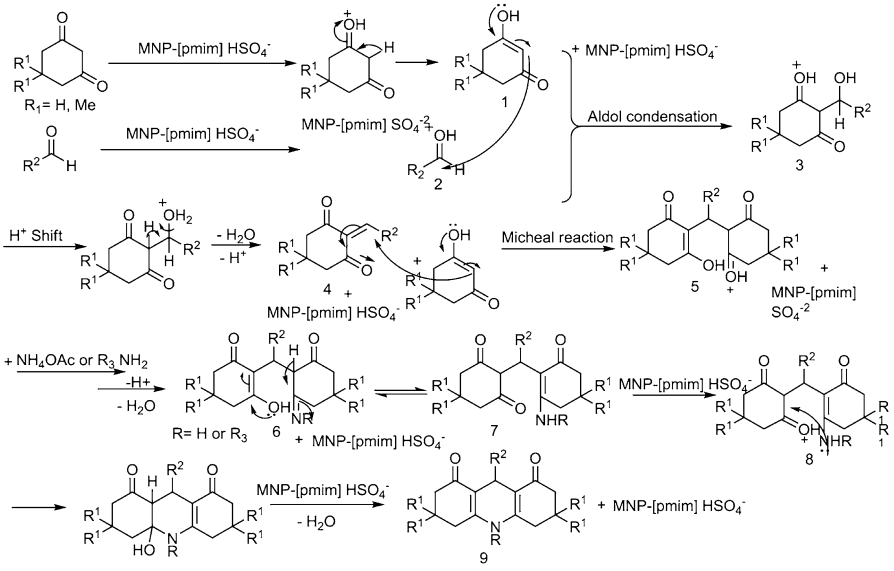

Scheme 3 Plausible mechanism for formation of acridines

carbonyl group of intermediate **5** could produce intermediate **6**. Intramolecular attack of nitrogen atom to activate carbonyl group followed by loss of water molecule affords acridine **9** as final product.

To show the merit of the present protocol for synthesis of 1,8-dioxodecahydroacridines, we compare our results with some reported in literature (Table 3).

Table 3 Comparison of the introduced methodology with some other reported methods

Entry	Catalyst (amount)	Reaction conditions	Yield (%)/time	Ref.
1	SiO_2-Pr-SO_3H (0.02 g)	120 °C/solvent-free	83/2 h	[38]
2	IL[a] (1 mol%)	Reflux H_2O	–(Xanthene)	[17]
3	PEG 400/CAN (5 mol%)	50 °C	96/4 h	[19]
4	Amberlyst-15 (0.2 g)	CH_3CN/reflux	81/5 h	[14]
5	[Hmim]TFA (0.1 g)	80 °C/solvent-free	86/4.5 h	[18]
6	Fe_3O_4-NP (10 mol%)	120 °C/solvent free	85/25 min	[39]
7	FSG-Hf$(NPf_2)_4$ (1 mol%)	EtOH/H_2O reflux	49/6 h	[40]
8	MNP-[pmim]HSO_4 (1 mol%)	80 °C/solvent free	97/10 min	This work

[a] Imidazolium salt containing perfluoroalkyl tail

Although all the methods are effective, the present procedure affords comparatively high yield of the product with catalyst reusability for at least nine consecutive runs without loss of activity.

Conclusions

We successfully synthesized a supported IL of 1-methyl-3-(trimethoxysilyl)propyl imidazolium hydrogen sulfate (MNP-[pmim]HSO_4) from readily available starting materials. It was applied as a magnetically recyclable heterogeneous catalyst for one-pot multicomponent synthesis of 1,8-dioxodecahydroacridines in excellent yields and short reaction times. It is notable that product separation and catalyst recycling were easy and simple with the assistance of an external magnet. Furthermore, the catalyst could be recovered and reused for nine cycles without significant degradation in activity.

Acknowledgments We are grateful to the University of Mazandaran Research Council for financial support of this work.

References

1. M. Nuchter, B. Ondruschka, A. Jungnickel, U. Muller, J. Phys. Org. Chem. **13**, 579 (2000)
2. A. Habibi, E. Seikhhosseini-Lori, A. Shockravi, Tetrahedron Lett. **50**, 1075 (2009)
3. A. Domling, Curr. Opin. Chem. Biol. **6**, 306 (2002)
4. E. McDonald, K. Jones, P.A. Brough, M.J. Drysdale, P. Workman, Curr. Top. Med. Chem. **6**, 1193 (2006)
5. J. Elguero, P. Goya, N. Jagerovic, A.M.S. Silva, Targets Heterocycl. Syst. **6**, 52 (2002)
6. K. Venkatesan, S.S. Pujari, K. Srinivasan, Synth. Commun. **39**, 228 (2008)
7. V. Klusa, Drugs Future **20**, 135 (1995)
8. E. Delfourne, C. Roubin, J. Bastide, J. Org. Chem. **65**, 5476 (2000)
9. M.G. Ferlin, C. Marzano, G. Chiarelotto, F. Baccichetti, F. Bordin, Eur. J. Med. Chem. **35**, 827 (2000)
10. G. Rewcastle, G.J. Atwell, D. Chambers, B.C. Baguley, W.A. Denny, J. Med. Chem. **29**, 472 (1986)
11. P. Shanmugasundaram, P. Murugan, V.T. Ramakrishnan, Heteroat. Chem. **7**, 17 (1996)
12. X.S. Wang, D.Q. Shi, Y.F. Zhang, S.H. Wang, S.J. Tu, S. Chin, J. Org. Chem. **68**, 430 (2004)

13. T.S. Jin, J.S. Zhang, T.T. Guo, A.Q. Wang, T.S. Li, Synthesis **12**, 2001 (2004)
14. B. Das, P. Thirupathi, V. Mahender, S. Reddy, Y.K. Rao, J. Mol. Catal. A Chem. **247**, 233 (2006)
15. S. Balalaie, F. Chadegan, F. Darviche, H.R. Bijanzadeh, Chin. J. Chem. **27**, 1953 (2009)
16. S.J. Tu, C.B. Miao, Y. Gao, Y.J. Feng, J.C. Feng, Chin. J. Chem. **20**, 703 (2002)
17. W. Shen, L.M. Wang, H. Tian, J. Tang, J.J. Yu, J. Fluor. Chem. **130**, 522 (2009)
18. M. Dabiri, M. Baghbanzadeh, E. Arzroomchilar, Catal. Commun. **9**, 939 (2008)
19. M. Kidwai, V. Bhatnagar, Tetrahedron Lett. **51**, 2700 (2010)
20. K. Niknam, F. Panahi, D. Saberi, M. Mohagheghnejad, J. Heterocycl. Chem. **47**, 292 (2010)
21. A. Daştan, A. Kulkarni, B. Török, Green Chem. **14**, 17 (2012)
22. P. Wasserscheid, W. Keim, Angew. Chem. Int. Ed. **39**, 3772 (2000)
23. E. Öchsner, M.J. Schneider, C. Meyer, M. Haumann, P. Wasserscheid, Appl. Catal. A Gen. **399**, 35 (2011)
24. A. Hasaninejad, A. Zare, M. Shekouhy, J.A. Rad, J. Comb. Chem. **12**, 844 (2010)
25. T. Selvam, A. Machoke, W. Schwieger, Appl. Catal. A Gen. **445–446**, 92 (2012)
26. Y.-H. Kim, S. Shin, H.-J. Yoon, J.W. Kim, J.K. Cho, Y.-S. Lee, Catal. Commun. **40**, 18 (2013)
27. B. Kaboudin, R. Mostafalu, T. Yokomatsu, Green Chem. **15**, 2266 (2013)
28. M.B. Gawande, P.S. Branco, R.S. Varma, Chem. Soc. Rev. **42**, 3371 (2013)
29. H.-J. Xu, X. Wan, Y.-Y. Shen, S. Xu, Y.-S. Feng, Org. Lett. **14**, 1210 (2012)
30. A. Chrobok, S. Baj, W. Pudło, A. Jarzębski, Appl. Catal. A Gen. **366**, 22 (2009)
31. M. Tajbakhsh, M. Farhang, R. Hosseinzadeh, Y. Sarrafi, RSC Adv. **4**, 23116 (2014)
32. M. Bagheri, M. Masteri-Farahani, M. Ghorbani, J. Magn. Magn. Mater. **327**, 58 (2013)
33. J.-H. Li, X.-C. Hu, Y.-X. Xie, Tetrahedron Lett. **47**, 9239 (2006)
34. X.S. Wang, M.M. Zhang, H. Jiang, D.Q. Shi, S.J. Tu, X.Y. Wei, Z.M. Zong, Synthesis **24**, 4187 (2006)
35. M. Kaya, Y. Yildirir, T. Türker, J. Heterocycl. Chem. **46**, 294 (2009)
36. S. Chandrasekhar, Y.S. Rao, L. Sreelakshmi, B. Mahipal, C.R. Reddy, Synthesis **11**, 1737 (2008)
37. A. Davoodnia, A. Khojastehnezhad, N. Tavakoli-Hoseini, Bull. Korean Chem. Soc. **32**, 2243 (2011)
38. G.M. Ziarani, A. Badie, M. Hassanzadeh, S. Mousavi, Arab. J. Chem. **8**, 54 (2014)
39. M.A. Ghasemzadeh, J. Safaei-Ghomi, H. Molaei, C. R. Chim. **15**, 969 (2012)
40. M. Hong, G. Xiao, J. Fluor. Chem. **144**, 7 (2012)